Gapless spin excitations in the superconducting state of a quasi-one-dimensional spin-triplet superconductor

Keith M. Taddei [1,*] Bing-Hua Lei [2] Michael A. Susner,[3] Hui-Fei Zhai,[4] Thomas J. Bullard,[5,6] Liurukara D. Sanjeewa,[7]
Qiang Zheng,[7] Athena S. Sefat,[7] Songxue Chi,[1] Clarina dela Cruz,[1] David J. Singh,[2,†] and Bing Lv [4,‡]

[1]*Neutron Scattering Division, Oak Ridge National Laboratory, Oak Ridge, Tennessee 37831, USA*
[2]*Department of Physics and Astronomy, University of Missouri, Missouri 65211, USA*
[3]*Materials and Manufacturing Directorate, Air Force Research Laboratory, Wright-Patterson Air Force Base, Ohio 45433, USA*
[4]*University of Texas at Dallas, Richardson, Texas 75080, USA*
[5]*Aerospace Systems Directorate, Air Force Research Laboratory, Wright-Patterson Air Force Base, Ohio 45433, USA*
[6]*UES, Incorporated, 4401 Dayton Xenia Road, Dayton, Ohio 45432, USA*
[7]*Materials Science Division, Oak Ridge National Laboratory, Oak Ridge, Tennessee 37831, USA*

Majorana zero modes form as intrinsic defects in an odd-orbital one-dimensional superconductor, thus motivating the search for such materials in the pursuit of Majorana physics. Here, we present combined experimental results and first-principles calculations which suggest that quasi-one-dimensional $K_2Cr_3As_3$ may be such a superconductor. Using inelastic neutron scattering we probe the dynamic spin susceptibilities of $K_2Cr_3As_3$ and $K_2Mo_3As_3$ and show the presence of antiferromagnetic spin fluctuations in both compounds. Below the superconducting transition, these fluctuations gap in $K_2Mo_3As_3$ but not in $K_2Cr_3As_3$. Using first-principles calculations, we show that these fluctuations likely arise from nesting on one-dimensional features of the Fermi surface. Considering these results we propose that while $K_2Mo_3As_3$ is a conventional superconductor, $K_2Cr_3As_3$ is likely a spin triplet, and consequently a topological superconductor.

To realize scalable quantum computers, new phenomena on which to base the qubit are needed—ones robust, with intrinsic entangled properties such as exist in certain topological phases [1–9]. Of the potential candidates, the Majorana zero mode (MZM) is one of the most promising due to its non-Abelian anyon statistics which are suited for braiding while also potentially allowing manipulation necessary for computation [10–15]. However, generating and observing MZMs have proven challenging due to their complex materials' requirements and chargeless nature. One proposed route to realize and localize MZM is with one-dimensional superconductors (SCs) whose pair operators are their own conjugate—"spinless" or spin-triplet odd-orbital SCs—this is the original toy model proposed by Kitaev [11].

Consequently, there is great interest in one-dimensional (1D) or quasi-1D (Q1D) systems which exhibit spin-triplet SC (TSC). However, such materials are extraordinarily rare with few compounds showing either property and still fewer with both. Nonetheless, several candidate materials have been found (including the Bechgaard salts and purple bronze) [16–18]. More recently, the discovery of the Q1D potential TSC $A_nH_{(2-n)x}TM_3As_3$ (with A = Na, K, Rb, or Cs, TM = Cr or Mo, and n = 1 or 2) family has provided another route to realize these exotic physics [19–28].

The $A_nH_{(2-n)x}TM_3As_3$ materials exhibit numerous novel properties, several of which evince TSC. These materials crystallize with a motif of Q1D TM_3As_3 tubes which give rise to strongly Q1D features such as Luttinger-liquid physics, Q1D Fermi surfaces (FSs), and highly anisotropic transport [19,20,26,29–32]. Enticingly, their SC state appears to be unconventional with an unexpectedly high upper critical field, nodes in the SC gap, and a proximity to a quantum critical point with suggestions of TSC due to a spontaneous magnetization below the SC transition (T_C), an angular-dependent upper critical field, ferromagnetic (FM) fluctuations, a T_C suppressed by nonmagnetic impurities, and findings of a leading TSC instability from theory [33–46]. In $K_2Cr_3As_3$ this scenario was recently strengthened by nuclear magnetic resonance (NMR) measurements which revealed the spin susceptibility remains finite through T_C, strongly suggesting TSC [46].

However, some debate about the superconducting state still remains due to reports of anti-FM (AFM) instabilities, proximity to a spin-glass state, and an $s^\pm$ gap symmetry [28,47,48]. This has led to a complicated landscape for these materials with numerous proximate magnetic, structural, and superconducting instabilities. Recently, it was proposed that the $K_2TM_3As_3$ family may straddle a boundary between unconventional SC in $K_2Cr_3As_3$ ($T_C \sim 6$ K) and multigap conventional electron-phonon (e-p) SC in $K_2Mo_3As_3$ ($T_C \sim$ 10 K), perhaps giving guidance to understand the disparate reported features [49]. Here, it was argued that understanding how superconductivity evolved between the two compounds

---

*Corresponding author: taddeikm@ornl.gov
†singhdj@missouri.edu
‡blv@utdallas.edu

would elucidate the role of the different instabilities in the SC pairing, particularly in determining whether spin fluctuations (SFs) competed with or supported the SC state in $K_2Cr_3As_3$ [49].

In this Letter, we assess the role of SFs in $K_2Cr_3As_3$ through comparing the dynamic spin susceptibilities of $K_2Cr_3As_3$ and $K_2Mo_3As_3$ using experimental probes and first-principles calculations. To start, inelastic neutron scattering (INS) experiments reveal SFs in both compounds above T_C which are consistent with incipient AFM order. Below T_C, we find that for $K_2Mo_3As_3$ a nonresonant spin gap opens while in $K_2Cr_3As_3$ no gap is observed, implying a difference in the compounds' SC states. Performing first-principles calculations, we find that the AFM SF can be explained by FS nesting on Q1D FSs. Consequently, we suggest that $K_2Mo_3As_3$ is an *e-p* SC whose low-energy SFs are suppressed by the opening of SC gaps on all FSs. Contrastingly, the lack of a spin gap in $K_2Cr_3As_3$ indicates that neither the AFM SFs nor the associated FSs participate in SC, leaving a single remaining FS which is favorable to FM SF-driven TSC, thus indicating FM-driven TSC in $K_2Cr_3As_3$.

Large powder samples of $K_2Cr_3As_3$ and $K_2Mo_3As_3$ were synthesized as reported previously [see the Supplemental Material (SM) for details] [19,26,47]. Neutron powder diffraction (NPD) was performed on the HB-2A diffractometer of Oak Ridge National Laboratory's (ORNL) High Flux Isotope Reactor (HFIR) and analyzed using FULLPROF [50,51]. INS was performed on the HB-3 and C-TAX triple-axis spectrometers of HFIR using fixed analyzer energies of 14.7 and 5 meV, respectively. Density functional theory (DFT) calculations were performed using the generalized gradient approximation of Perdew, Burke, and Ernzerhof (PBE) and the general potential linearized augmented plane-wave method as implemented in the WIEN2K code [52–54].

In Fig. 1(a) we show the crystal structure of $K_2Mo_3As_3$ (space group $P\bar{6}m2$) which exhibits a Q1D structural motif of two inequivalent, alternating, coaxial layers of Mo (and As) triangles. In Fig. 1(b) we show a diffraction pattern of $K_2Mo_3As_3$ collected at 300 K together with a simulated pattern from our best-fit model showing no impurity phase, indicating the high quality of our sample. In the inset of Fig. 1(b) we show a comparison of NPD patterns collected at 300 and 2 K demonstrating a lack of any significant changes which might be associated with the onset of magnetic order suggesting $K_2Mo_3As_3$ (as $K_2Cr_3As_3$) has no long-range magnetic order (see the SM for more discussion) [55].

Previously, $K_2Cr_3As_3$ was shown to have AFM SFs arising from incipient $\mathbf{k} = (0, 0, \frac{1}{2})$ order. This was revealed as a column of scattering in the dynamic structure factor $S(q, \Delta E)$ (as probed via INS) which is proportional to the imaginary component of the spin susceptibility [47,56,57]. Such fluctuations offer significant insights to the SC state, therefore we performed similar experiments on $K_2Mo_3As_3$ and compare these materials' $S(Q, \Delta E)$.

Figures 2(a) and 2(c) show the $S(Q, \Delta E)$ of $K_2Mo_3As_3$ and $K_2Cr_3As_3$ collected at 20 and 10 K, respectively (above either compound's T_C). Here, we focus on the low Q and low ΔE region which is typically featureless at these temperatures for nonmagnetic materials. However, for both materials a column of scattering is seen arising from ∼0.75 Å^{-1}. Such
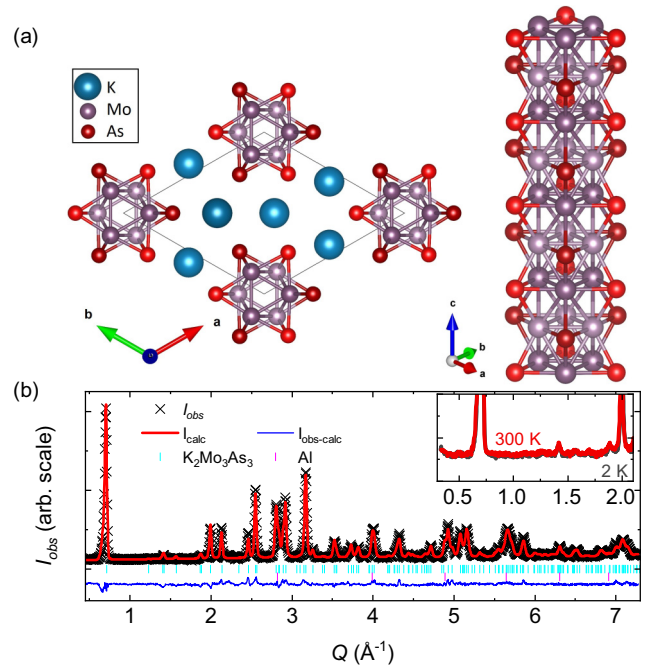

FIG. 1. (a) Crystal structure of $K_2Mo_3As_3$ viewed along c and of the isolated tube motif. (b) Neutron powder diffraction pattern and best-fit model for data collected at 300 K. The inset of (b) shows a comparison of the low Q region of data collected at 300 and 2 K.

a signal is often indicative of incipient magnetic order caused by SFs with a Q characteristic of the incipient ordering vector [39,57–61].

Qualitatively, the signal observed in $K_2Mo_3As_3$ is similar to that of $K_2Cr_3As_3$. Fitting constant ΔE cuts with Gaussian functions, we find a slight shift in the position of the feature to lower Q by ∼0.1 Å^{-1} in $K_2Mo_3As_3$ compared to $K_2Cr_3As_3$, consistent with $K_2Mo_3As_3$'s larger c axis (see SM for details) [55]. The dispersion of the two signals is very similar (though both are convoluted with the instrument resolution function). On the other hand, the fits reveal that the column in $K_2Mo_3As_3$ is broader in Q by ∼20% and also is ∼30% weaker (though this is more difficult to reliably quantify between samples), which may indicate the fluctuations are shorter ranged and the fluctuating moment smaller in $K_2Mo_3As_3$, both of which have been suggested from prior DFT treatments [49]. Due to these considerations, we attribute the origin of this signal to similar causes as in $K_2Cr_3As_3$.

We next consider the temperature dependencies across T_C. Figures 2(b) and 2(d) show the same region of $S(Q, \Delta E)$ measured below T_C at 2 K for both samples. Here, a distinction between the two emerges. For $K_2Cr_3As_3$ the spectrograph looks qualitatively identical to the 20-K data set—no gap opens despite the onset of SC. On the other hand, in $K_2Mo_3As_3$ [Fig. 2(b)] there is a clear change in the column where the signal for $\Delta E < 7$ meV loses intensity. This observation is consistent with the opening of a SC gap which inhibits fluctuations below 2Δ (i.e., the energy required to break a Cooper pair).

To characterize this feature, constant Q scans were taken at $Q \sim 1.1$ Å^{-1} above and below T_C for both samples (Fig. 3). For $K_2Mo_3As_3$ [Fig. 3(a)], the gap becomes clear. While

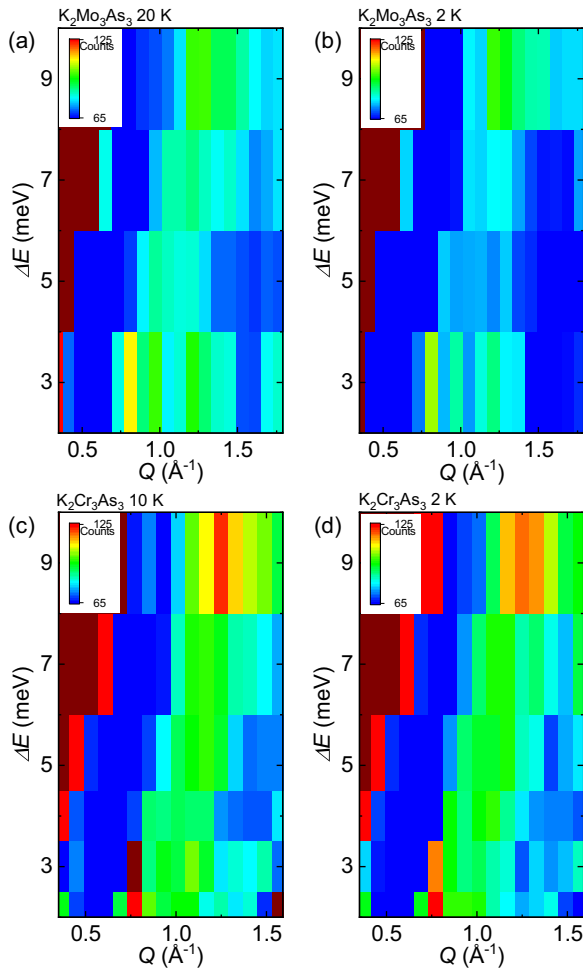FIG. 2. Inelastic neutron scattering spectrograms for $K_2Mo_3As_3$ at (a) 20 K and (b) 2 K and for $K_2Cr_3As_3$ at (c) 10 K and (d) 2 K. Intensity is in units of detector counts normalized to monitor counts. We note that the data showed in (c) include data from Ref. [47] but with additional counting statistics.

FIG. 3. (a) Comparison of scattering intensity of $K_2Mo_3As_3$ for constant q scans along the column collected at 20 and 2 K. (b) Temperature dependence of the low-energy region of the $K_2Mo_3As_3$ column with the 20 K count rate and T_C denoted by horizontal and vertical dotted lines. (c) Difference curve for the 20- and 2-K $K_2Mo_3As_3$ data using a larger ΔE bin size than (a) to improve the statistics. (d) Similar comparison of 20- and 2-K scans for $K_2Cr_3As_3$ with an envelope denoting the size of a gap expected for a signal similar to that observed in (a).

the 20-K data exhibit a constant increase in intensity below 5 meV (as the elastic line is approached), the 2-K data drop in intensity by $\sim$20% below $\sim$5 meV. Using the weak coupling Bardeen-Cooper-Schieffer gap approximation [i.e., $\Delta(T = 0) = \frac{7}{2}k_BT_C$] we estimate 2Δ as 6.2 meV, which is consistent with our observed gap (a similar estimate is obtained using the empirical formula of $\omega_0 = 4.3k_BT_c$ with ω_0 being the energy of the spin gap) [62]. In Fig. 3(c) we show a difference curve of the 20- and 2-K data to remove background effects. Here, the gap is seen to open below $\sim$5 meV and progressively widen to the lowest measured temperature of 2 K. We further associate this gap with T_C by measuring the intensity at 1.05 Å^{-1} and 3 meV as a function of temperature [Fig. 3(b)] which shows the gap to close at $\sim$6 K. This is a little below T_C (10.4 K); however, the gap itself is a function of T and so should become smaller than the certainty of our measurements before T_C is exceeded.

In $K_2Cr_3As_3$, we see discretely different behavior in the low-energy spectrum [Fig. 3(d)]. Here, no obvious SF gap is seen in the 2-K data. If estimated as before, $2\Delta \sim 3.7$ meV and $\omega_0 \sim 2.2$ meV, both of which are within the limits of our
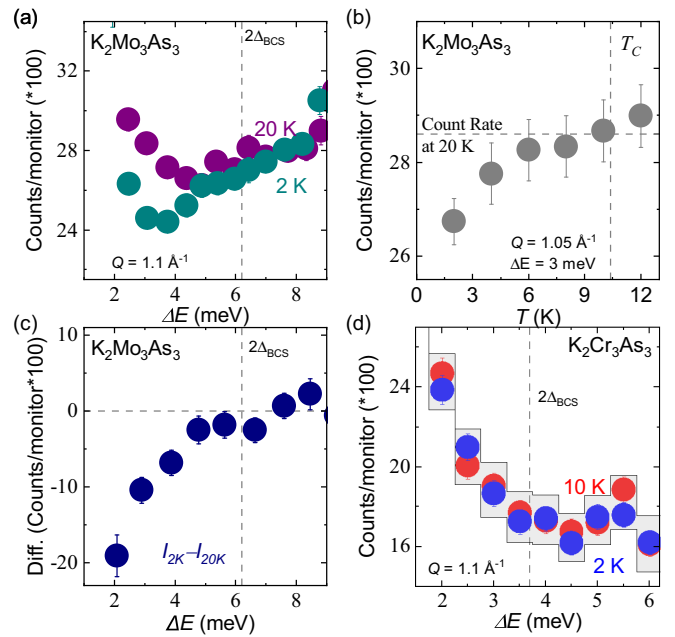
energy resolution ($\sim$1.4 meV). For comparison, in Fig. 3(d) we plot an envelope showing the range equivalent to the percent change of the signal seen in $K_2Mo_3As_3$, demonstrating that, within our statistics, a similar decrease in intensity would be observable. Additional measurements were taken using a cold neutron triple-axis spectrometer to access lower-energy transfers ($<$1 meV) and no gap was observed (see SM) [55]. Consequently, we take this observation to be a strong indication that no spin gap opens in the SC state of $K_2Cr_3As_3$.

Such observations have significant implications for the nature of SC in these systems [49]. That the SFs in $K_2Cr_3As_3$ do not respond strongly to SC (which naively should open a gap) requires explanation. Furthermore, though a spin gap with a resonance has become a hallmark of unconventional SCs, here we see no evidence of a resonance above the gap in $K_2Mo_3As_3$ undermining the SF role in SC [63]. If the SFs can be associated with specific features of the FSs, then the presence (or absence) of a gap in those SFs will correspond to the presence (or absence) of a gap on the associated FS. In a system such as $K_2Cr_3As_3$, where different FSs have different SC instabilities, such information can be key in determining the symmetry of the SC state [62,64–76].

In Figs. 4(a) and 4(b) we show the FSs of $K_2Mo_3As_3$ and (undistorted) $K_2Cr_3As_3$ as determined by DFT calculations. Here, we use undistorted $K_2Cr_3As_3$ due to ambiguity in the distorted structure [77,78]. As reported, these two compounds have similar FSs, consisting of two Q1D α and β sheets and one large three-dimensional (3D) γ sheet [40,43,49,79–81].
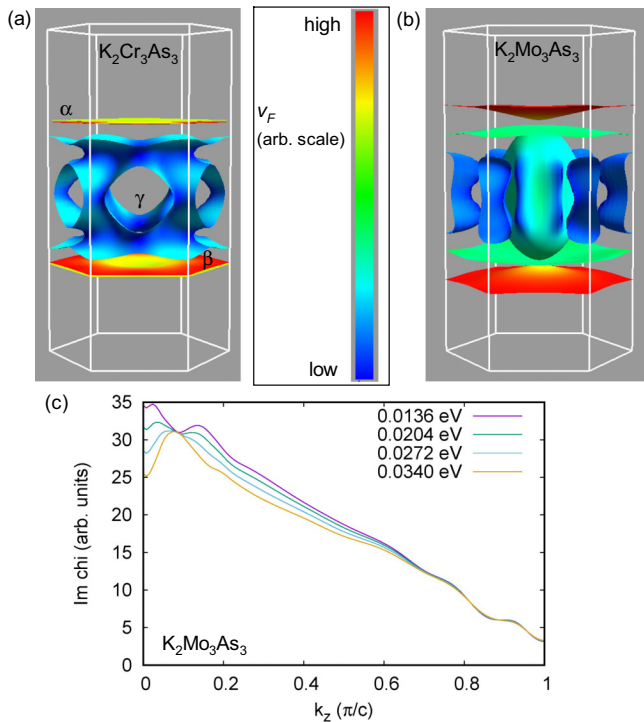
FIG. 4. Calculated Fermi surfaces of (a) $K_2Cr_3As_3$ (undistorted) and (b) $K_2Mo_3As_3$. In (a) and (b) the calculated Fermi velocity is shown as a function of position on the Fermi surface via the color scale with blue indicating low relative velocities and red indicating higher velocities. (c) Imaginary component of the calculated Lindhard susceptibility of $K_2Mo_3As_3$ plotted for several energies near the Fermi energy (with $E_F = 0$ eV).

Given the large sheetlike features of the FSs, nesting vectors have been proposed as possible between both the upper and lower α and β sheets as well as between the top and bottom of the γ sheet, any of which may lead to spin- or charge-density-wave type orders such as have been proposed for the SFs observed in $K_2Cr_3As_3$ [39,47,49,78,82,83].

We next calculate the Fermi velocities (v_F) throughout the FSs of both compounds to predict the strength of electron correlations on the different surfaces [as shown in the color scale on Figs. 4(a) and 4(b)]. These calculations reveal two important features: For both compounds the large 3D γ sheet has significantly lower v_F, indicating stronger electron correlations (and magnetic interactions) on this sheet. Additionally, v_F is in general larger in $K_2Mo_3As_3$, suggesting it exhibits weaker electron correlations than $K_2Cr_3As_3$.

If there is an electronic instability to nesting between the Q1D FSs, then we expect an associated peak in the dynamic spin susceptibility as calculated via the imaginary component of the Lindhard susceptibility [shown projected along k_z for $K_2Mo_3As_3$ in Fig. 4(c)]. Here, we clearly observe a large broad peak near the zone center indicative of FM SFs as has been previously suggested in prior first-principles studies [43,80,84,85]. Such a signal is consistent with the experimental evidence for FM SFs found in NMR measurements [35,46,58,86]. Near the zone boundary at $k_z \sim 0.9$, we see a second feature which corresponds to the **k** position of the

AFM SFs observed in INS. This peak is quite small, consistent with it arising from nesting between the two high v_F Q1D sheets, and similar to prior observations in $A_2Cr_3As_3$ and ACr_3As_3 [43,83,87,88].

These insights from first-principles provide a roadmap to interpret the experimental results. They show that both $K_2Mo_3As_3$ and $K_2Cr_3As_3$ have similar potential nesting vectors across the 1D FSs, consistent with the observed column of SFs. That these AFM SFs do not gap in $K_2Cr_3As_3$ indicates that neither the AFM SFs nor the 1D FSs participate in SC. This is expected as symmetry considerations for AFM SF-mediated spin-singlet or spin-triplet SC disallow Cooper pairs between k_z and $-k_z$ states [89,90]. In $K_2Mo_3As_3$ the SF gap do not exhibit a resonant-spin excitation which further contradicts AFM SF-driven SC [83]. The ungapped Q1D FSs in $K_2Cr_3As_3$ imply SC must exist on the γ sheet. Given that FM SC can pair k and $-k$ states for a sign changing gap, as occurs in the proposed p_z-wave symmetry, this allows a possible scenario for a TSC mechanism [39,89]. We note that our experimental results cannot eliminate other possible pairing potentials which might be available on the γ sheet, however, they do weaken e-p as a candidate, which is inconsistent with the presence of an ungapped FS [49]. Furthermore, for FM SFs the pairing potential is enhanced for low scattering vectors as found on the γ surface which encompasses the zone center, consistent with the low v_F found on this sheet and in additional support of TSC [89].

Considering previous experimental reports of FM SFs and the recent report of TSC which have largely been driven by NMR experiments, our INS results provide important insights. Whereas the previously reported SFs were argued to possibly arise from combinations of AFM and FM components which obfuscated their relevance in pairing, here we clearly show that in $K_2Cr_3As_3$ the AFM SFs do not participate in SC [58]. Additionally, our results are consistent with the recently proposed scenario of a proximate FM quantum critical point (QCP) in the Cr compounds [35]. Here, tuning away from the QCP gives rise to residual FM SFs which in turn can drive TSC pairing [35,91]. On the other hand, while our results are complimentary to the recent NMR observation of a finite spin susceptibility inside the SC state and subsequent identification of TSC, our symmetry analysis suggests a p_z symmetry rather than the $(p_x \pm ip_y)$, indicating the need for additional experimental evaluation of the SC gap structure [46]. More generally, that both AFM and FM SFs exist in $K_2Cr_3As_3$ but only the latter responds to SC is highly suggestive of TSC. However, localizing SC to the 3D γ sheet undermines arguments for 1D SC, instead encouraging the use of $K_2Cr_3As_3$ as a material with TSC, which still requires macroscopic manipulation of sample shape to achieve a 1D wire geometry. Nevertheless, our results are consistent with a p_z-wave TSC state in $K_2Cr_3As_3$ and encourage further work, potentially pointing to a system which advantageously TSC and a highly Q1D crystal habit may help with device design as well as in isolating such states [83,92,93].

In summary, we show that both $K_2Cr_3As_3$ and $K_2Mo_3As_3$ exhibit antiferromagnetic spin fluctuations which are consistent with an incipient **k** $= (0, 0, \frac{1}{2})$ type magnetic order. Comparing spectra collected above and below their respective T_C's, we find that while $K_2Mo_3As_3$ exhibits a gap with no

spin resonance, $K_2Cr_3As_3$ exhibits no such gap. Using first-principles calculations, we show that these two materials are susceptible to nesting across their Q1D Fermi surfaces, consistent with the experimental $\mathbf{k} = (0, 0, \frac{1}{2})$. As we observe no gap in the spin fluctuations of $K_2Cr_3As_3$, we infer that these Fermi surfaces are not gapped by the superconducting state and that the remaining γ sheet, which should favor spin-triplet pairing, must host superconductivity. Furthermore, we rule out the antiferromagnetic coupling superconducting mechanism in $K_2Cr_3As_3$, leaving ferromagnetic fluctuation-driven spin-triplet superconductivity as the lead candidate mechanism. As $K_2Cr_3As_3$ is a Q1D material, its hosting spin-triplet superconductivity should have exciting implications for topological physics invoking aspects of Kitaev's toy model for Majorana zero modes.

[1] F. Arute, K. Arya, R. Babbush, D. Bacon, J. C. Bardin, R. Barends, R. Biswas, S. Boixo, F. G. Brandao, D. A. Buell *et al.*, Quantum supremacy using a programmable superconducting processor, Nature (London) **574**, 505 (2019).

[2] C. J. Ballance, T. P. Harty, N. M. Linke, M. A. Sepiol, and D. M. Lucas, High-Fidelity Quantum Logic Gates Using Trapped-Ion Hyperfine Qubits, Phys. Rev. Lett. **117**, 060504 (2016).

[3] M. H. Devoret and R. J. Schoelkopf, Superconducting circuits for quantum information: an outlook, Science **339**, 1169 (2013).

[4] M. R. Geller, E. J. Pritchett, A. T. Sornborger, and F. Wilhelm, Quantum computing with superconductors I: Architectures, in *Manipulating Quantum Coherence in Solid State Systems* (Springer, Berlin, 2007), pp. 171–194.

[5] K. D. Petersson, J. R. Petta, H. Lu, and A. C. Gossard, Quantum Coherence in a One-Electron Semiconductor Charge Qubit, Phys. Rev. Lett. **105**, 246804 (2010).

[6] A. Y. Kitaev, Fault-tolerant quantum computation by anyons, Ann. Phys. **303**, 2 (2003).

[7] C. Nayak, S. H. Simon, A. Stern, M. Freedman, and S. Das Sarma, Non-Abelian anyons and topological quantum computation, Rev. Mod. Phys. **80**, 1083 (2008).

[8] A. Stern and N. H. Lindner, Topological quantum computation—from basic concepts to first experiments, Science **339**, 1179 (2013).

[9] N. P. de Leon, K. M. Itoh, D. Kim, K. K. Mehta, T. E. Northup, H. Paik, B. Palmer, N. Samarth, S. Sangtawesin, and D. Steuerman, Materials challenges and opportunities for quantum computing hardware, Science **372**, eabb2823 (2021).

[10] C. Beenakker, Search for Majorana fermions in superconductors, Annu. Rev. Condens. Matter Phys. **4**, 113 (2013).

[11] A. Y. Kitaev, Unpaired Majorana fermions in quantum wires, Phys. Usp. **44**, 131 (2001).

[12] S. Vaitiekėnas, G. W. Winkler, B. van Heck, T. Karzig, M.-T. Deng, K. Flensberg, L. I. Glazman, C. Nayak, P. Krogstrup, R. M. Lutchyn *et al.*, Flux-induced topological superconductivity in full-shell nanowires, Science **367**, eaav3392 (2020).

[13] F.-L. Xiong, H.-L. Lai, and W.-M. Zhang, Manipulating Majorana qubit states without braiding, Phys. Rev. B **104**, 205417 (2021).

[14] J. Alicea, Y. Oreg, G. Refael, F. Von Oppen, and M. P. Fisher, Non-Abelian statistics and topological quantum information processing in 1D wire networks, Nat. Phys. **7**, 412 (2011).

[15] C. Tutschku, R. W. Reinthaler, C. Lei, A. H. MacDonald, and E. M. Hankiewicz, Majorana-based quantum computing in nanowire devices, Phys. Rev. B **102**, 125407 (2020).

[16] S. Brown, Organic superconductors: The Bechgaard salts and relatives, Phys. C: Supercond. **514**, 279 (2015).

[17] W. Cho, C. Platt, R. H. McKenzie, and S. Raghu, Spin-triplet superconductivity in a weak-coupling Hubbard model for the quasi-one-dimensional compound $Li_{0.9}Mo_6O_{17}$, Phys. Rev. B **92**, 134514 (2015).

[18] I. A. Firmo, S. Lederer, C. Lupien, A. P. Mackenzie, J. C. Davis, and S. A. Kivelson, Evidence from tunneling spectroscopy for a quasi-one-dimensional origin of superconductivity in Sr_2RuO_4, Phys. Rev. B **88**, 134521 (2013).

[19] J.-K. Bao, J.-Y. Liu, C.-W. Ma, Z.-H. Meng, Z.-T. Tang, Y.-L. Sun, H.-F. Zhai, H. Jiang, H. Bai, C.-M. Feng, Z.-A. Xu, and G.-H. Cao, Superconductivity in Quasi-One-Dimensional $K_2Cr_3As_3$, Phys. Rev. X **5**, 011013 (2015).

[20] J.-K. Bao, L. Li, Z.-T. Tang, Y. Liu, Y.-K. Li, H. Bai, C.-M. Feng, Z.-A. Xu, and G.-H. Cao, Cluster spin-glass ground state in quasi-one-dimensional KCr_3As_3, Phys. Rev. B **91**, 180404(R) (2015).

[21] J.-J. Xiang, Y.-L. Yu, S.-Q. Wu, B.-Z. Li, Y.-T. Shao, Z.-T. Tang, J.-K. Bao, and G.-H. Cao, Superconductivity induced by aging and annealing in $K_{1-\delta}Cr_3As_3H_x$, Phys. Rev. Mater. **3**, 114802 (2019).

[22] Z.-T. Tang, J.-K. Bao, Y. Liu, Y.-L. Sun, A. Ablimit, H.-F. Zhai, H. Jiang, C.-M. Feng, Z.-A. Xu, and G.-H. Cao, Unconventional

superconductivity in quasi-one-dimensional $Rb_2Cr_3As_3$, Phys. Rev. B **91**, 020506(R) (2015).

[23] Z.-T. Tang, J.-K. Bao, Z. Wang, H. Bai, H. Jiang, Y. Liu, and H.-F. Zhai, Superconductivity in quasi-one-dimensional $Cs_2Cr_3As_3$ with large interchain distance, Sci. China Mater. **58**, 16 (2015).

[24] Z.-T. Tang, J. Bao, Y. Liu, H. Bai, H. Jiang, H.-F. Zhai, C.-M. Feng, Z.-A. Xu, and G.-H. Cao, Synthesis, crystal structure and physical properties of quasi-one-dimensional ACr_3As_3 (A = Rb, Cs), Sci. China Mater. **58**, 543 (2015).

[25] Q.-G. Mu, B.-B. Ruan, B.-J. Pan, T. Liu, J. Yu, K. Zhao, G.-F. Chen, and Z.-A. Ren, Ion-exchange synthesis and superconductivity at 8.6 K of $Na_2Cr_3As_3$ with quasi-one-dimensional crystal structure, Phys. Rev. Mater. **2**, 034803 (2018).

[26] Q.-G. Mu, B.-B. Ruan, K. Zhao, B.-J. Pan, T. Liu, L. Shan, G.-F. Chen, and Z.-A. Ren, Superconductivity at 10.4 K in a novel quasi-one-dimensional ternary molybdenum pnictide $K_2Mo_3As_3$, Sci. Bull. **63**, 952 (2018).

[27] T. Liu, Q.-G. Mu, B.-J. Pan, J. Yu, B.-B. Ruan, K. Zhao, G.-F. Chen, and Z.-A. Ren, Superconductivity at 7.3 K in the 133-type Cr-based single crystals, Europhys. Lett. **120**, 27006 (2017).

[28] K. M. Taddei, L. D. Sanjeewa, B.-H. Lei, Y. Fu, Q. Zheng, D. J. Singh, A. S. Sefat, and C. dela Cruz, Tuning from frustrated magnetism to superconductivity in quasi-one-dimensional KCr_3As_3 through hydrogen doping, Phys. Rev. B **100**, 220503(R) (2019).

[29] G. Cao, J.-K. Bao, Z.-T. Tang, Y. Liu, and H. Jiang, Peculiar properties of Cr_3As_3 chain-based superconductors, Philos. Mag. **97**, 591 (2017).

[30] Q.-G. Mu, B.-B. Ruan, B.-J. Pan, T. Liu, J. Yu, K. Zhao, G.-F. Chen, and Z.-A. Ren, Superconductivity at 5 K in quasi-one-dimensional Cr-based KCr_3As_3 single crystals, Phys. Rev. B **96**, 140504(R) (2017).

[31] C. Noce, The chromium pnictide materials: A tunable platform for exploring new exciting phenomena, Europhys. Lett. **130**, 67001 (2020).

[32] M. D. Watson, Y. Feng, C. W. Nicholson, C. Monney, J. M. Riley, H. Iwasawa, K. Refson, V. Sacksteder, D. T. Adroja, J. Zhao, and M. Hoesch, Multiband One-Dimensional Electronic Structure and Spectroscopic Signature of Tomonaga-Luttinger Liquid Behavior in $K_2Cr_3As_3$, Phys. Rev. Lett. **118**, 097002 (2017).

[33] F. F. Balakirev, T. Kong, M. Jaime, R. D. McDonald, C. H. Mielke, A. Gurevich, P. C. Canfield, and S. L. Bud'ko, Anisotropy reversal of the upper critical field at low temperatures and spin-locked superconductivity in $K_2Cr_3As_3$, Phys. Rev. B **91**, 220505(R) (2015).

[34] G. M. Pang, M. Smidman, W. B. Jiang, J. K. Bao, Z. F. Weng, Y. F. Wang, L. Jiao, J. L. Zhang, G. H. Cao, and H. Q. Yuan, Evidence for nodal superconductivity in quasi-one-dimensional $K_2Cr_3As_3$, Phys. Rev. B **91**, 220502(R) (2015).

[35] J. Luo, J. Yang, R. Zhou, Q. G. Mu, T. Liu, Z.-a. Ren, C. J. Yi, Y. G. Shi, and G.-q. Zheng, Tuning the Distance to a Possible Ferromagnetic Quantum Critical Point in $A_2Cr_3As_3$, Phys. Rev. Lett. **123**, 047001 (2019).

[36] D. T. Adroja, A. Bhattacharyya, M. Telling, Y. Feng, M. Smidman, B. Pan, J. Zhao, A. D. Hillier, F. L. Pratt, and A. M. Strydom, Superconducting ground state of quasi-one-dimensional $K_2Cr_3As_3$ investigated using μSR measurements, Phys. Rev. B **92**, 134505 (2015).

[37] Y. Liu, J.-K. Bao, H.-K. Zuo, A. Ablimit, Z.-T. Tang, C.-M. Feng, Z.-W. Zhu, and G.-H. Cao, Effect of impurity scattering on superconductivity in $K_2Cr_3As_3$, Sci. China: Phys., Mech. Astron. **59**, 657402 (2016).

[38] H. Zuo, J.-K. Bao, Y. Liu, J. Wang, Z. Jin, Z. Xia, L. Li, Z. Xu, J. Kang, Z. Zhu, and G.-H. Cao, Temperature and angular dependence of the upper critical field in $K_2Cr_3As_3$, Phys. Rev. B **95**, 014502 (2017).

[39] H. Z. Zhi, T. Imai, F. L. Ning, J.-K. Bao, and G.-H. Cao, NMR Investigation of the Quasi-One-Dimensional Superconductor $K_2Cr_3As_3$, Phys. Rev. Lett. **114**, 147004 (2015).

[40] X.-X. Wu, F. Yang, C. Le, H. Fan, and J.-P. Hu, Triplet p_z-wave pairing in quasi-one-dimensional $A_2Cr_3As_3$ superconductor, Phys. Rev. B **92**, 104511 (2015).

[41] H. Zhong, X.-Y. Feng, H. Chen, and J. Dai, Formation of Molecular-Orbital Bands in a Twisted Hubbard Tube: Implications for Unconventional Superconductivity in $K_2Cr_3As_3$, Phys. Rev. Lett. **115**, 227001 (2015).

[42] L.-D. Zhang, X.-X. Wu, H. Fan, F. Yang, and J.-P. Hu, Revisitation of superconductivity in $K_2Cr_3As_3$ based on the six-band model, Europhys. Lett. **113**, 37003 (2016).

[43] C. Xu, N. Wu, G.-X. Zhi, B.-H. Lei, X. Duan, F. Ning, C. Cao, and Q. Chen, Coexistence of nontrivial topological properties and strong ferromagnetic fluctuations in quasi-one-dimensional $A_2Cr_3As_3$, npj Comput. Mater. **6**, 30 (2020).

[44] S.-Q. Wu, C. Cao, and G.-H. Cao, Lifshitz transition and nontrivial H-doping effect in the Cr-based superconductor $KCr_3As_3H_x$, Phys. Rev. B **100**, 155108 (2019).

[45] G. Cuono, F. Forte, A. Romano, X. Ming, J. Luo, C. Autieri, and C. Noce, Intrachain collinear magnetism and interchain magnetic phases in Cr_3As_3-K-based materials, Phys. Rev. B **103**, 214406 (2021).

[46] J. Yang, J. Luo, C. Yi, Y. Shi, Y. Zhou, and G.-q. Zheng, Spin-triplet superconductivity in $K_2Cr_3As_3$, Sci. Adv. **7**, eabl4432 (2021).

[47] K. M. Taddei, Q. Zheng, A. S. Sefat, and C. de la Cruz, Coupling of structure to magnetic and superconducting orders in quasi-one-dimensional $K_2Cr_3As_3$, Phys. Rev. B **96**, 180506(R) (2017).

[48] C. Cao, H. Jiang, X.-Y. Feng, and J. Dai, Reduced dimensionality and magnetic frustration in KCr_3As_3, Phys. Rev. B **92**, 235107 (2015).

[49] B.-H. Lei and D. J. Singh, Multigap electron-phonon superconductivity in the quasi-one-dimensional pnictide $K_2Mo_3As_3$, Phys. Rev. B **103**, 094512 (2021).

[50] S. Calder, K. An, R. Boehler, C. Dela Cruz, M. Frontzek, M. Guthrie, B. Haberl, A. Huq, S. A. Kimber, J. Liu *et al.*, A suite-level review of the neutron powder diffraction instruments at oak ridge national laboratory, Rev. Sci. Instrum. **89**, 092701 (2018).

[51] J. Rodríguez-Carvajal, Recent advances in magnetic structure determination by neutron powder diffraction, Phys. B: Condens. Matter **192**, 55 (1993).

[52] J. P. Perdew, K. Burke, and M. Ernzerhof, Generalized Gradient Approximation Made Simple, Phys. Rev. Lett. **77**, 3865 (1996).

[53] D. Singh and L. Nordström, *Planewaves, Pseudopotentials and the LAPW Method*, 2nd ed. (Springer, Berlin, 2006).

[54] P. Blaha, K. Schwarz, F. Tran, R. Laskowski, G. K. H. Madsen, and L. D. Marks, WIEN2k: An APW+lo program for calculating the properties of solids, J. Chem. Phys. **152**, 074101 (2020).

[55] See Supplemental Material at http://link.aps.org/supplemental/10.1103/PhysRevB.107.L180504 for details pertaining to sample synthesis, diffraction data collection, Rietveld refinements. and a more in-depth discussion of the DFT results.

[56] I. Zaliznyak and S. Lee, Magnetic Neutron Scattering (OSTI, 2004), https://www.osti.gov/biblio/15009517.

[57] L. M. Whitt, T. C. Douglas, S. Chi, K. M. Taddei, and J. M. Allred, Magnetic excitation linking quasi-one-dimensional Chevrel-type selenide and arsenide superconductors, Phys. Rev. Mater. **6**, 124804 (2022).

[58] H. Zhi, D. Lee, T. Imai, Z. Tang, Y. Liu, and G. Cao, ^{133}Cs and ^{75}As NMR investigation of the normal metallic state of quasi-one-dimensional $Cs_2Cr_3As_3$, Phys. Rev. B **93**, 174508 (2016).

[59] M. C. Rahn, R. A. Ewings, S. J. Sedlmaier, S. J. Clarke, and A. T. Boothroyd, Strong $(\pi, 0)$ spin fluctuations in β-FeSe observed by neutron spectroscopy, Phys. Rev. B **91**, 180501(R) (2015).

[60] A. E. Taylor, M. J. Pitcher, R. A. Ewings, T. G. Perring, S. J. Clarke, and A. T. Boothroyd, Antiferromagnetic spin fluctuations in LiFeAs observed by neutron scattering, Phys. Rev. B **83**, 220514(R) (2011).

[61] Z. Wang, W. Yi, Q. Wu, V. A. Sidorov, J. Bao, Z. Tang, J. Guo, Y. Zhou, S. Zhang, H. Li, Y. Shi, X. Wu, L. Zhang, K. Yang, A. Li, G. Cao, J. Hu, L. Sun, and Z. Zhao, Correlation between superconductivity and bond angle of CrAs chain in non-centrosymmetric compounds $A_2Cr_3As_3$ (A = K, Rb), Sci. Rep. **6**, 37878 (2016).

[62] A. D. Christianson, E. A. Goremychkin, R. Osborn, S. Rosenkranz, M. D. Lumsden, C. D. Malliakas, I. S. Todorov, H. Claus, D. Y. Chung, M. G. Kanatzidis, R. I. Bewley, and T. Guidi, Unconventional superconductivity in $Ba_{0.6}K_{0.4}Fe_2As_2$ from inelastic neutron scattering, Nature (London) **456**, 930 (2008).

[63] G. R. Stewart, Unconventional superconductivity, Adv. Phys. **66**, 75 (2017).

[64] T. E. Mason, G. Aeppli, and H. A. Mook, Magnetic Dynamics of Superconducting $La_{1.86}Sr_{0.14}CuO_4$, Phys. Rev. Lett. **68**, 1414 (1992).

[65] T. Dahm, D. Manske, and L. Tewordt, Collective modes in high-temperature superconductors, Phys. Rev. B **58**, 12454 (1998).

[66] P. Dai, H. A. Mook, S. M. Hayden, G. Aeppli, T. G. Perring, R. D. Hunt, and F. Doğan, The magnetic excitation spectrum and thermodynamics of high-T_c superconductors, Science **284**, 1344 (1999).

[67] S. Chi, A. Schneidewind, J. Zhao, L. W. Harriger, L. Li, Y. Luo, G. Cao, Z. Xu, M. Loewenhaupt, J. Hu, and P. Dai, Inelastic Neutron-Scattering Measurements of a Three-Dimensional Spin Resonance in the FeAs-Based $BaFe_{1.9}Ni_{0.1}As_2$ Superconductor, Phys. Rev. Lett. **102**, 107006 (2009).

[68] R. Osborn, S. Rosenkranz, E. Goremychkin, and A. Christianson, Inelastic neutron scattering studies of the spin and lattice dynamics in iron arsenide compounds, Phys. C: Supercond. **469**, 498 (2009).

[69] J. T. Park, G. Friemel, Y. Li, J.-H. Kim, V. Tsurkan, J. Deisenhofer, H.-A. Krug von Nidda, A. Loidl, A. Ivanov, B. Keimer, and D. S. Inosov, Magnetic Resonant Mode in the Low-Energy Spin-Excitation Spectrum of Superconduct-

[70] N. Qureshi, P. Steffens, Y. Drees, A. C. Komarek, D. Lamago, Y. Sidis, L. Harnagea, H.-J. Grafe, S. Wurmehl, B. Büchner, and M. Braden, Inelastic Neutron-Scattering Measurements of Incommensurate Magnetic Excitations on Superconducting LiFeAs Single Crystals, Phys. Rev. Lett. **108**, 117001 (2012).

[71] D. J. Scalapino, A common thread: The pairing interaction for unconventional superconductors, Rev. Mod. Phys. **84**, 1383 (2012).

[72] C. Zhang, R. Yu, Y. Su, Y. Song, M. Wang, G. Tan, T. Egami, J. A. Fernandez-Baca, E. Faulhaber, Q. Si, and P. Dai, Measurement of a Double Neutron-Spin Resonance and an Anisotropic Energy Gap for Underdoped Superconducting $NaFe_{0.985}Co_{0.015}As$ Using Inelastic Neutron Scattering, Phys. Rev. Lett. **111**, 207002 (2013).

[73] J. M. Tranquada, G. Xu, and I. A. Zaliznyak, Superconductivity, antiferromagnetism, and neutron scattering, J. Magn. Magn. Mater. **350**, 148 (2014).

[74] Q. Wang, Y. Shen, B. Pan, Y. Hao, M. Ma, F. Zhou, P. Steffens, K. Schmalzl, T. Forrest, M. Abdel-Hafiez et al., Strong interplay between stripe spin fluctuations, nematicity and superconductivity in FeSe, Nat. Mater. **15**, 159 (2016).

[75] T. Xie, D. Gong, H. Ghosh, A. Ghosh, M. Soda, T. Masuda, S. Itoh, F. Bourdarot, L.-P. Regnault, S. Danilkin et al., Neutron Spin Resonance in the 112-Type Iron-Based Superconductor, Phys. Rev. Lett. **120**, 137001 (2018).

[76] S. Kunkemöller, P. Steffens, P. Link, Y. Sidis, Z. Q. Mao, Y. Maeno, and M. Braden, Absence of a Large Superconductivity-Induced Gap in Magnetic Fluctuations of Sr_2RuO_4, Phys. Rev. Lett. **118**, 147002 (2017).

[77] K. M. Taddei, G. Xing, J. Sun, Y. Fu, Y. Li, Q. Zheng, A. S. Sefat, D. J. Singh, and C. de la Cruz, Frustrated Structural Instability in Superconducting Quasi-One-Dimensional $K_2Cr_3As_3$, Phys. Rev. Lett. **121**, 187002 (2018).

[78] G. Xing, L. Shang, Y. Fu, W. Ren, X. Fan, W. Zheng, and D. J. Singh, Structural instability and magnetism of superconducting KCr_3As_3, Phys. Rev. B **99**, 174508 (2019).

[79] P. Alemany and E. Canadell, Links between the crystal and electronic structure in the new family of unconventional superconductors $A_2Cr_3As_3$ (A = K, Rb, Cs), Inorg. Chem. **54**, 8029 (2015).

[80] H. Jiang, G. Cao, and C. Cao, Electronic structure of quasi-one-dimensional superconductor $K_2Cr_3As_3$ from first-principles calculations, Sci. Rep. **5**, 16054 (2015).

[81] Y. Yang, S.-Q. Feng, H.-Y. Lu, W.-S. Wang, and Z.-P. Chen, Electronic Structures of Newly Discovered Quasi-One-Dimensional Superconductors $A_2Mo_3As_3$ (A= K, Rb, Cs), J. Supercond. Novel Magn. **32**, 2421 (2019).

[82] A. Subedi, Strong-coupling electron-phonon superconductivity in noncentrosymmetric quasi-one-dimensional $K_2Cr_3As_3$, Phys. Rev. B **92**, 174501 (2015).

[83] L.-D. Zhang, X. Zhang, J.-J. Hao, W. Huang, and F. Yang, Singlet $s^{\pm}$-wave pairing in quasi-one-dimensional ACr_3As_3 (A = K, Rb, Cs) superconductors, Phys. Rev. B **99**, 094511 (2019).

[84] Ž. Gosar, N. Janša, T. Arh, P. Jeglič, M. Klanjšek, H. F. Zhai, B. Lv, and D. Arčon, Superconductivity in the regime of attractive interactions in the Tomonaga-Luttinger liquid, Phys. Rev. B **101**, 220508(R) (2020).

[85] S. Raymond, Magnetic excitations, Ec. Them. Soc. Fr. Neutron. **13**, 02003 (2014).

[86] J. Yang, Z. T. Tang, G. H. Cao, and G.-q. Zheng, Ferromagnetic Spin Fluctuation and Unconventional Superconductivity in $Rb_2Cr_3As_3$ Revealed by ^{75}As NMR and NQR, Phys. Rev. Lett. **115**, 147002 (2015).

[87] J. P. Lu, Q. Si, J. H. Kim, and K. Levin, NMR Relaxation and Neutron Scattering in a Fermi-Liquid Picture of the Metallic Copper Oxides, Phys. Rev. Lett. **65**, 2466 (1990).

[88] G. T. Wang, Y. Qian, G. Xu, X. Dai, and Z. Fang, Gutzwiller Density Functional Studies of FeAs-Based Superconductors: Structure Optimization and Evidence for a Three-Dimensional Fermi Surface, Phys. Rev. Lett. **104**, 047002 (2010).

[89] I. I. Mazin and D. J. Singh, Ferromagnetic Spin Fluctuation Induced Superconductivity in Sr_2RuO_4, Phys. Rev. Lett. **79**, 733 (1997).

[90] M. Sigrist, Introduction to unconventional superconductivity, in *Lectures on the Physics of Highly Correlated Electron Systems*, edited by A. Avella and F. Mancini, AIP Conf. Proc. Vol. 789 (American Institute of Physics, Melville, NY, 2005), pp. 165–243.

[91] S. Ran, C. Eckberg, Q.-P. Ding, Y. Furukawa, T. Metz, S. R Saha, I-L. Liu, M. Zic, H. Kim, J. Paglione, and others, Nearly ferromagnetic spin-triplet superconductivity, Science **365**, 684 (2019).

[92] X.-X. Wu, C.-C. Le, J. Yuan, H. Fan, and J.-P. Hu, Magnetism in Quasi-One-Dimensional $A_2Cr_3As_3$ (A = K,Rb) Superconductors, Chin. Phys. Lett. **32**, 057401 (2015).

[93] C.-C. Liu, C. Lu, L.-D. Zhang, X. Wu, C. Fang, and F. Yang, Intrinsic topological superconductivity with exactly flat surface bands in the quasi-one-dimensional $A_2Cr_3As_3$ (A = Na, K, Rb, Cs) superconductors, Phys. Rev. Res. **2**, 033050 (2020).

[94] http://energy.gov/downloads/doe-public-access-plan.